

On bottom friction in an equatorial shallow basin

Roger L. HUGHES (1)

ABSTRACT

Observations of the flow on the Sunda Shelf near Singapore do not agree with the flow modelled using a depth integrated numerical model. The discrepancy, which takes place in a western boundary current, is consistent with an equatorial irregularity in the bottom stress. This irregularity may be explained in terms of the influence of equatorial upwelling within the bottom boundary layer distorting the structure of that layer. This structural variation is such as to introduce a mean westward bottom stress correction on water crossing the equator irrespective of the manner in which the equator is crossed.

KEY WORDS : Equatorial — Shallow water — Bottom stress — Sunda shelf.

RÉSUMÉ

RÔLE DU FROTTEMENT SUR LE FOND DANS UN BASSIN ÉQUATORIAL PEU PROFOND

Les observations du courant sur le plateau continental de la Sonde, à proximité de Singapour, ne concordent pas avec les résultats d'un modèle numérique de circulation intégrée sur toute l'épaisseur. La discordance que l'on note sur le bord ouest du courant peut être mise en relation avec l'anomalie équatoriale de la tension de frottement sur le fond. On peut expliquer cette anomalie en prenant en considération la déformation de la structure de la couche de fond par l'upwelling équatorial. Cette déformation induit une correction qui tend à renforcer la partie ouest du courant franchissant l'Équateur, quel que soit le sens de ce franchissement.

MOTS-CLÉS : Équatorial — Bassin peu profond — Frottement sur le fond — Plateau de la Sonde.

1. INTRODUCTION

The Sunda Shelf is extremely important to both the fishing industry of Indonesia and the shipping industry associated with the busy port of Singapore. It contains the only major shallow cross-equatorial channel flow. The mean depth of the shelf is of the order of 70 m. Fig. 1 shows the observed cross-equatorial surface flow as indicated by WYRTKI (1961). It can be seen that the flow reverses with the monsoonal season. From December to April, the northwesterly monsoon blows the water to the

south. From June to August the southeasterly monsoon blows the water to the north. The observational background associated with fig. 1 is small. However, there appears to be an unmistakable concentration of the flow on the western boundary irrespective of the direction of the flow. This current lies very close to Singapore and its proper identification may have significant economic benefits.

GROVES and NIEMEYER (1975) have numerically modelled the flow in the entire Sunda Shelf. The model they used contained a staggered grid finite difference representation of the time dependent

(1) Australian Numerical Meteorology Research Centre, Melbourne, Vic. 3001, Australia.

(Present address: Department of Geology and Geophysics, Yale University, P.O. Box 6666, New Haven, CT 06511, USA).

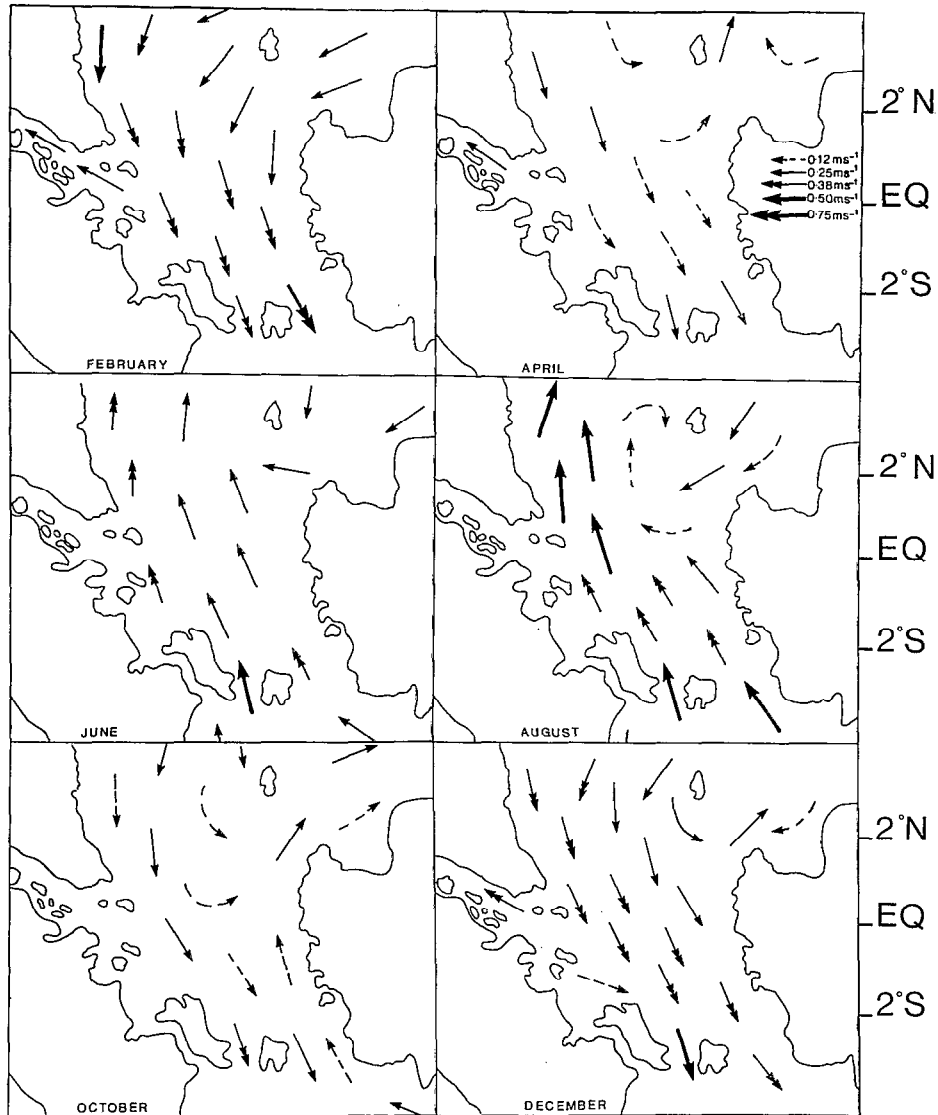


FIG. 1. — Observed surface circulation on the equatorial Sunda Shelf between Borneo and Sumatra for February, April, June, August, October and December as given by WYRTKI (1961). Notice the slight tendency for the current to be concentrated on the western boundary when crossing the equator.

Circulation de surface observée dans la partie équatoriale du plateau de la Sonde, entre Bornéo et Sumatra, en février, avril, juin, août, octobre et décembre, selon WYRTKI (1961). Noter la légère tendance du courant à s'intensifier à l'Ouest, lors du passage de l'Équateur.

shallow water equations. Linearity was assumed throughout except in the representation of bottom friction which was of standard quadratic form. Full allowance was made for the variable bottom topography of the Sunda Shelf. At coastlines the normal velocity was set to zero (no restriction on the tangential velocity was required because of the lack of a horizontal diffusion in the model). At the open boundaries, which were located just off the shelf, the surface elevation was fixed. The model

was forced by the wind stress alone. The numerical procedure was based on the HANSEN (1962) method, (see GROVES and NIEMEYER for details). The grid resolution was of the order of 50 km and was stepped with a time increment of approximately 7 minutes for 25 days of real time. Results from their depth averaged model for the two monsoonal seasons are shown in fig. 2. It can be seen that while the general character of the flow is the same as the surface flow as given by WYRTKI (1961),

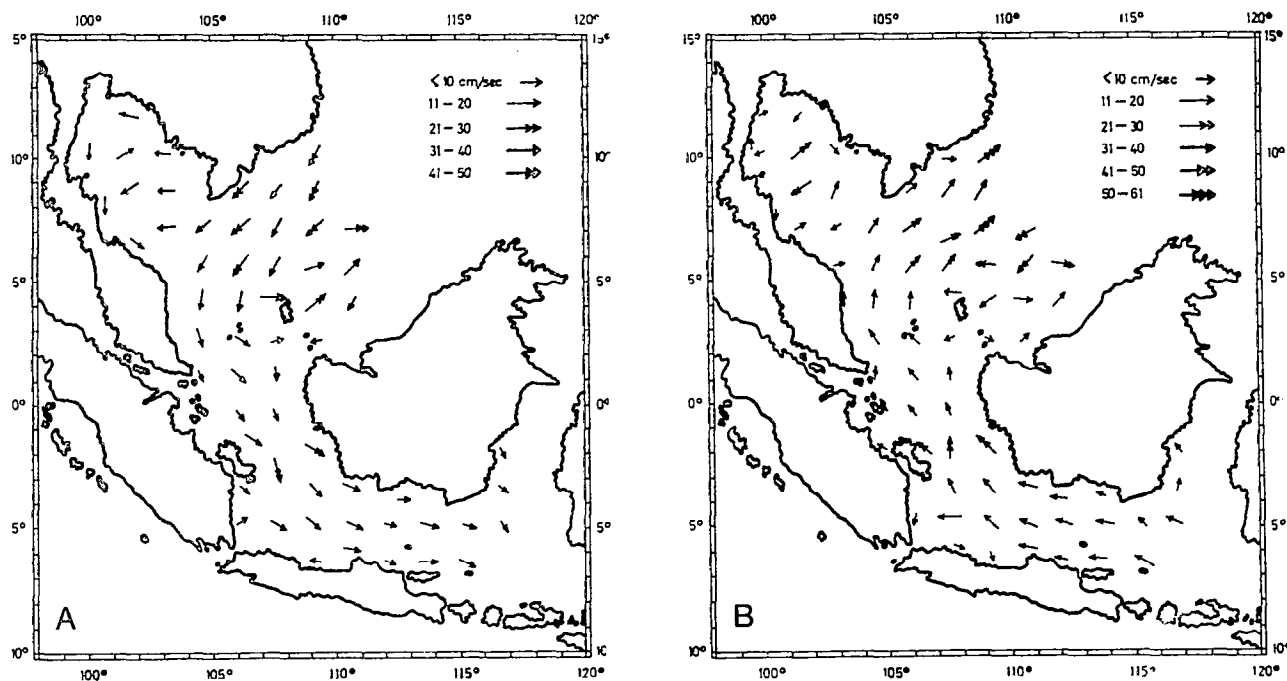


FIG. 2. — Flow determined numerically by GROVES and NIEMEYER (1975) using the usual formulation of bottom stress. Case A is for the Northwest Monsoon. Case B is for the Southeast Monsoon. No tendency for currents to concentrate near the western boundary while crossing the equator is observed

Courant résultant du modèle numérique utilisant la formulation classique des tensions de fond, selon GROVES et NIEMEYER (1975). A : en période de mousson de Nord-Ouest ; B : en période de mousson de Sud-Est. Aucune tendance du courant à s'intensifier à l'Ouest lors du passage de l'Équateur

there is no suggestion of a western boundary current near the equator. Three possible reasons for this discrepancy are :

1—WYRTKI's data were too sparse to justify the conclusion drawn above. This seems unlikely especially given the accuracy with which WYRTKI (1961) has shown for some of the other seas of the area where further observations seem to be supporting theories based upon his observations.

2—There is a substantial difference between the surface flow and the depth averaged flow. If this were correct, it would imply a reverse flow at depth at some locations in the western part of the equatorial Sunda Shelf. Such a reversal is possible if the flow is driven by a strong pressure gradient as well as the monsoonal wind. However, this explanation seems extremely unlikely as such a reversal would almost certainly have been mentioned in the literature, which to the author's knowledge it has not.

3—Some effect not allowed for in the model of GROVES and NIEMEYER (1975) is significant. There is a commonly neglected effect which becomes important at low latitudes. This is the secondary

circulation, in particular how it effects the bottom stress. The effect is investigated here.

We define the secondary circulation to be the frictionally induced transverse circulation across the channel (that is in the plane orthogonal to the depth integrated flow). HSUEH and O'BRIEN (1971) give a good account of a secondary circulation induced by bottom friction. In that case the circulation is driven by a mismatch in geostrophic balance in the frictionally controlled lower boundary layer. In equatorial latitudes where the Coriolis parameter is small, the secondary circulation induced by that mechanism is apparently small and dominated by the mechanism given here.

Fig. 3 gives a diagrammatic representation of a possible secondary circulation. In the interior of the basin's bottom boundary layer Ekman pumping (applicable at middle and high latitudes) or β -divergence (applicable at low latitudes) causes a vertical velocity. A return flow occurs through the interior, the side boundary layer and bottom boundary layer in turn as found by HSUEH and O'BRIEN (1971). As will be seen later the vertical velocity induced by β -divergence is of the order of U_s where U

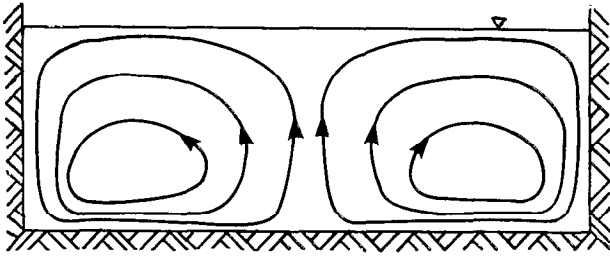


FIG. 3. — Idealized cross-section through a basin showing the likely form of secondary circulation in response to Ekman pumping at the lower boundary. Whether there is upwelling or downwelling associated with the Ekman pumping depends on the case being studied. It is unclear whether one of the boundaries dominates the other in returning the flow. See HSUEH and O'BRIEN (1971) for an example.

Coupe schématique d'un bassin montrant la structure de la circulation secondaire engendrée par le pompage d'Ekman au niveau de la couche profonde. Un upwelling ou un downwelling est, selon le cas, associé avec le pompage d'Ekman. Le rôle prépondérant de l'une ou de l'autre des limites du bassin, lorsque le sens du flux s'inverse, n'est pas évident. Voir un exemple dans HSUEH et O'BRIEN (1971).

and s are respectively the characteristic horizontal velocity and a flow independent non-dimensional parameter which obtains a maximum value near the equator of about 10^{-5} . The associated horizontal velocity in the flow interior and bottom boundary layer are of the order of $U_s \frac{L_x}{L_z}$ and $U_s \frac{L_x}{L_B}$ respectively

where L_x , L_z and L_B are characteristic of the horizontal, vertical and boundary layer distance scales. If L_B , $L_z \sim 35$ m and $L_x \sim 5 \times 10^5$ m as is appropriate here, it follows that for the equatorial region of the Sunda Shelf, the magnitude of the horizontal velocity associated with the secondary circulation is probably near to being an order of magnitude less than that of the basic flow. Hence the horizontal velocity associated with the secondary circulation can be neglected. However, the effect of the vertical velocity on the bottom boundary layer and hence the bottom shear stress controlling the depth integrated flow cannot necessarily be ignored.

Although not the centre of interest to this study, it is interesting to note that unusual bottom stresses have been observed by SCOTT and CSANADY (1976), FORRISTALL *et al.* (1977) and SMITH (1978). Various ideas have been put forward to explain these observations. However, to the author's knowledge, no uniformly satisfactory theory has been given. No theory based on the influence of the secondary circulation induced by nearby storms has been considered.

2. THE IMPORTANCE OF MID-LATITUDE FRICTIONALLY INDUCED UPWELLING

Before considering equatorial latitudes, it is useful to consider a simple model of the boundary layer applicable to non-equatorial latitudes. Although the predicted flow may be unstable to rolls, the classical Ekman layer model is of such simplicity that it is used here (GREENSPAN, 1969; BARCILON, 1965). The case considered here is of an Ekman layer in a flow with (horizontally) locally uniform vertical vorticity.

$$\text{This is to say } \left(\frac{\partial}{\partial x}, \frac{\partial}{\partial y} \right) \left(\frac{\partial v}{\partial x} - \frac{\partial u}{\partial y} \right) = 0, \quad (2.1)$$

locally where (u, v, w) represents the velocity field. The classical Ekman layer as commonly presented is imbedded in a flow of zero vertical vorticity.

The equations governing the steady motion in the Ekman layer are

$$w \frac{\partial u}{\partial z} - fv = - \frac{\partial p}{\partial x} + \kappa \frac{\partial^2 u}{\partial z^2} \quad (2.2)$$

$$w \frac{\partial v}{\partial z} + fu = - \frac{\partial p}{\partial y} + \kappa \frac{\partial^2 v}{\partial z^2} \quad (2.3)$$

$$\frac{\partial u}{\partial x} + \frac{\partial v}{\partial y} + \frac{\partial w}{\partial z} = 0, \quad (2.4)$$

where p , f and κ are respectively the kinematic pressure, constant Coriolis parameter and constant vertical eddy viscosity. Distances measured upwards from the bottom boundary are denoted by positive z . At large distances from the boundary layer (2.2) and (2.3) reduce to the usual geostrophic relations

$$-fv_\infty = - \frac{\partial p}{\partial x} \quad (2.5)$$

$$fu_\infty = - \frac{\partial p}{\partial y}, \quad (2.6)$$

where $(u_\infty, v_\infty, w_\infty)$ denotes the far field velocity of which only the first two components are specified.

As is usual in boundary layer theory $\frac{\partial p}{\partial x}$ and $\frac{\partial p}{\partial y}$ are

assumed to be constant throughout the boundary layer depth. The third component of the far field velocity, w_∞ , is given by the Ekman pumping requirement which is a consistency requirement on (2.2) to (2.4). If (2.2) and (2.3) are linearised this requirement is

$$w_\infty = \frac{\kappa}{f} \left[\frac{\partial}{\partial z} \left(\frac{\partial v}{\partial x} - \frac{\partial u}{\partial y} \right) \right] \Big|_{z=0} \quad (2.7)$$

Thus the boundary conditions on (2.2) and (2.4) are

$$u, v, w = 0 \quad \text{at } z = 0 \quad (2.8)$$

$$u, v \rightarrow u_\infty, v_\infty \quad \text{as } z \rightarrow \infty. \quad (2.9)$$

Eq. (2.2) - (2.4) form a non-linear set of equations which in the present study is best solved by a perturbation expansion. As suggested by (2.7), we write

$$\begin{aligned} u &= u_0 + \varepsilon u_1 + \varepsilon^2 u_2 \dots \\ v &= v_0 + \varepsilon v_1 + \varepsilon^2 v_2 \dots \\ w &= \varepsilon w_1 + \varepsilon^2 w_2 \dots \end{aligned} \tag{2.10}$$

where ε is the expansion parameter (representing the non-dimensional vorticity) given by

$$\varepsilon = \frac{1}{f} \left(\frac{\partial v_\infty}{\partial x} - \frac{\partial u_\infty}{\partial y} \right), \tag{2.11}$$

which is characteristically much less than unity in magnitude for most non-equatorial oceanographic situations.

Zeroth order terms

To order ε^0 , (2.2) and (2.3) can be written as

$$-f(v_0 - v_\infty) = \kappa \frac{\partial^2 (u_0 - u_\infty)}{\partial z^2} \tag{2.12}$$

$$f(u_0 - u_\infty) = \kappa \frac{\partial^2 (v_0 - v_\infty)}{\partial z^2} \tag{2.13}$$

for which the solution satisfying (2.8) and (2.9) is the classical Ekman spiral,

$$u_0 = u_\infty - \exp(-Z) (u_\infty \cos(Z) + v_\infty \sin(Z)) \tag{2.14}$$

$$v_0 = v_\infty - \exp(-Z) (v_\infty \cos(Z) - u_\infty \sin(Z)), \tag{2.15}$$

where $Z = \sqrt{\frac{f}{2\kappa}} z$ for the northern hemisphere.

This solution constituting the classical Ekman spiral, is illustrated and compared with observations by POLLARD (1977).

First order terms

After a little manipulation (2.2)-(2.4) can be combined to give an equation for w ; this being

$$w \frac{\partial}{\partial z} \left[\kappa \frac{\partial^3 w}{\partial z^3} - w \frac{\partial^2 w}{\partial z^2} \right] - f^2 \frac{\partial w}{\partial z} = \kappa \frac{\partial^2}{\partial z^2} \left[\kappa \frac{\partial^3 w}{\partial z^3} - w \frac{\partial^2 w}{\partial z^2} \right]. \tag{2.16}$$

From this equation it can be shown that to order ε^1 , w is given by

$$\varepsilon w_1 = \frac{1}{f} \left(\frac{\partial v_\infty}{\partial x} - \frac{\partial u_\infty}{\partial y} \right) \sqrt{\frac{\kappa f}{2}} (1 - \exp(-Z) (\cos(Z) + \sin(Z))). \tag{2.17}$$

It follows from (2.2) and (2.3) that the corrections to u and v at order ε are

$$\begin{aligned} \varepsilon u_1 &= \frac{1}{f} \left(\frac{\partial v_\infty}{\partial x} - \frac{\partial u_\infty}{\partial y} \right) (-Z \exp(-Z) (u_\infty \cos(Z) + v_\infty \sin(Z)) \\ &\quad - \frac{1}{3} \exp(-2Z) (u_\infty \cos(2Z) + v_\infty \sin(2Z)) + \frac{1}{5} \\ &\quad (v_\infty - 2u_\infty) \exp(-2Z) \end{aligned}$$

$$\begin{aligned} &- \exp(-Z) \left(\left(-\frac{u_\infty}{3} + \frac{v_\infty - 2u_\infty}{5} \right) \cos(Z) + \right. \\ &\left. \left(-\frac{v_\infty}{3} - \frac{u_\infty + 2v_\infty}{5} \right) \sin(Z) \right) \end{aligned} \tag{2.18}$$

$$\begin{aligned} \varepsilon v_1 &= \frac{1}{f} \left(\frac{\partial v_\infty}{\partial x} - \frac{\partial u_\infty}{\partial y} \right) (-Z \exp(-Z) (v_\infty \cos(Z) - \\ &u_\infty \sin(Z)) \\ &\quad - \frac{1}{3} \exp(-2Z) (v_\infty \cos(2Z) - u_\infty \sin(2Z)) - \\ &\quad \frac{1}{5} (u_\infty + 2v_\infty) \exp(-2Z) \end{aligned}$$

$$\begin{aligned} &- \exp(-Z) \left(\left(-\frac{v_\infty}{3} - \frac{u_\infty + 2v_\infty}{5} \right) \cos(Z) - \right. \\ &\left. \left(-\frac{u_\infty}{3} + \frac{v_\infty - 2u_\infty}{5} \right) \sin(Z) \right) \end{aligned} \tag{2.19}$$

A complicated decaying spiral is the predicted form of the correction induced by upwelling. The overall distance scale of this correction is of the same order as that of the Ekman spiral itself.

The correction to the bottom stress (τ_x , τ_y), is given by

$$\begin{aligned} \varepsilon \tau_{x1} &= -\kappa \frac{\partial \varepsilon u_1}{\partial z} \Big|_{z=0} = -\frac{1}{f} \left(\frac{\partial v_\infty}{\partial x} - \frac{\partial u_\infty}{\partial y} \right) \left(-\frac{u_\infty}{15} \right. \\ &\left. - \frac{2v_\infty}{15} \right) \sqrt{\frac{f\kappa}{2}} \end{aligned} \tag{2.20}$$

$$\begin{aligned} \varepsilon \tau_{y1} &= -\kappa \frac{\partial \varepsilon v_1}{\partial z} \Big|_{z=0} = -\frac{1}{f} \left(\frac{\partial v_\infty}{\partial x} - \frac{\partial u_\infty}{\partial y} \right) \left(-\frac{v_\infty}{15} \right. \\ &\left. + \frac{2u_\infty}{15} \right) \sqrt{\frac{f\kappa}{2}} \end{aligned} \tag{2.21}$$

There is substantial veering in the correction, just as there is for the conventional Ekman spiral (although the direction is opposite). Of more importance, the correction to the shear stress is of order $\varepsilon/10$ times the shear stress without the upwelling allowance. This correction is generally negligible in non-equatorial latitudes for which the model is applicable. If the model were valid in the neighbourhood of the equator the correction would dominate the solution. However, it is not valid there, and it is only suggestive of the importance of the mechanism to this region.

3. THE IMPORTANCE OF LOW-LATITUDE FRICTIONALLY INDUCED UPWELLING

Having established that the change in bottom stress caused by upwelling within the bottom boundary layer is only likely to be commonly significant at low latitudes, it is constructive to model this region. Because low latitude upwelling is dominated by β -induced divergence rather than vorticity induced Ekman pumping, it is convenient to consider a vorticity free far field flow. Thus

$$\frac{\partial v}{\partial x} - \frac{\partial u}{\partial y} = 0 \quad (3.1)$$

locally. The basic dynamical equations of the previous section (2.2)-(2.4), and the geostrophic relations, (2.5) and (2.6), remain valid at low latitudes although f is no longer constant but is given by βy in accordance with the equatorial β -plane used here. (The equator is excluded from consideration to avoid a singularity located there. Later a Rayleigh friction is introduced to eliminate this difficulty but its inclusion at this stage is cumbersome). An expansion of the form (2.10) is applicable where ε is now given by

$$\varepsilon = \left(\frac{u_{\infty}^2 + v_{\infty}^2}{\beta y^2} \right)^{1/2} \quad (3.2)$$

rather than (2.11). The boundary conditions (2.8) and (2.9) remain valid.

Zeroth order terms

To order ε^0 the solution is a classical Ekman spiral

$$u_0 = u_{\infty} - \exp(-Z) (u_{\infty} \cos(Z) + v_{\infty} \sin(Z)) \quad (3.3)$$

$$v_0 = v_{\infty} - \exp(-Z) (v_{\infty} \cos(Z) - u_{\infty} \sin(Z)) \quad (3.4)$$

where $Z = \sqrt{\frac{\beta y}{2\kappa}} z$ for the northern hemisphere.

Notice that the vertical distance scale of the spiral becomes unbounded as the equator is approached.

First order terms

As the model is locally x -independent the continuity equation (2.4), reduces to

$$\frac{\partial w}{\partial z} = - \frac{\partial v}{\partial y} \quad (3.5)$$

Thus to order ε^1 , w is given by

$$\begin{aligned} \varepsilon w_1 = & \sqrt{\frac{\kappa}{2\beta y^3}} \left(\frac{1}{2} (u_{\infty} - v_{\infty}) + \exp(-Z) (v_{\infty} Z \cos(Z) - u_{\infty} Z \sin(Z)) \right. \\ & \left. - \frac{1}{2} (u_{\infty} - v_{\infty}) \cos(Z) - \frac{1}{2} (u_{\infty} + v_{\infty}) \sin(Z) \right) \quad (3.6) \end{aligned}$$

and hence from (2.2.) and (2.3) the corrections to u and v at order ε^1 are

$$\begin{aligned} \varepsilon u_1 = & \frac{1}{\beta y^2} \left(\exp(-Z) \left(\left(\frac{41}{900} u_{\infty}^2 + \frac{391}{900} v_{\infty}^2 + \frac{8}{175} u_{\infty} v_{\infty} \right) \cos(Z) \right. \right. \\ & \left. \left. + \left(\frac{7}{100} (u_{\infty}^2 + v_{\infty}^2) + \frac{47}{150} u_{\infty} v_{\infty} \right) \sin(Z) \right) \right. \\ & \left. - \frac{1}{4} (u_{\infty}^2 - u_{\infty} v_{\infty}) Z \cos(Z) + \frac{1}{4} (v_{\infty}^2 - u_{\infty} v_{\infty}) Z \sin(Z) \right) \end{aligned}$$

$$\begin{aligned} & + \exp(-2Z) \left(-\frac{6}{25} (u_{\infty}^2 + v_{\infty}^2) - \frac{3}{20} (u_{\infty}^2 + v_{\infty}^2) Z \right) \\ & + \frac{1}{12} \left(v_{\infty}^2 + \frac{8}{5} u_{\infty} v_{\infty} - u_{\infty}^2 \right) Z \cos(2Z) \\ & + \frac{1}{12} \left(-u_{\infty}^2 - 2 u_{\infty} v_{\infty} + v_{\infty}^2 \right) Z \sin(2Z) \\ & + \left(\frac{7}{36} v_{\infty}^2 - \frac{7}{36} u_{\infty}^2 - \frac{8}{175} u_{\infty} v_{\infty} \right) \cos(2Z) - \\ & \frac{53}{150} u_{\infty} v_{\infty} \sin(2Z) \quad (3.7) \end{aligned}$$

$$\begin{aligned} \varepsilon v_1 = & \frac{1}{\beta y^2} \left(\exp(-Z) \left(\left(\frac{7}{100} (u_{\infty}^2 + v_{\infty}^2) + \frac{47}{150} u_{\infty} v_{\infty} \right) \cos(Z) \right. \right. \\ & \left. \left. - \left(\frac{41}{900} u_{\infty}^2 + \frac{391}{900} v_{\infty}^2 + \frac{8}{175} u_{\infty} v_{\infty} \right) \sin(Z) \right) \right. \\ & \left. + \frac{1}{4} (v_{\infty}^2 - u_{\infty} v_{\infty}) Z \cos(Z) + \frac{1}{4} (u_{\infty}^2 - u_{\infty} v_{\infty}) Z \sin(Z) \right) \\ & + \exp(-2Z) \left(-\frac{7}{100} (u_{\infty}^2 + v_{\infty}^2) + \frac{1}{20} (u_{\infty}^2 + v_{\infty}^2) Z \right. \\ & \left. + \frac{1}{12} (v_{\infty}^2 - 2 u_{\infty} v_{\infty} - u_{\infty}^2) Z \cos(2Z) \right. \\ & \left. - \frac{1}{12} (v_{\infty}^2 + \frac{2}{5} u_{\infty} v_{\infty} - u_{\infty}^2) Z \sin(2Z) \right. \\ & \left. - \frac{47}{150} u_{\infty} v_{\infty} \cos(2Z) + \left(\frac{7}{36} u_{\infty}^2 - \frac{7}{36} v_{\infty}^2 + \frac{17}{175} u_{\infty} v_{\infty} \right) \sin(2Z) \right) \quad (3.8) \end{aligned}$$

As in the previous section the correction to u and v is a spiral having the same distance scale as the basic Ekman spiral.

The correction to the bottom stress (τ_x , τ_y), is calculated as in the previous section. It is now given by

$$\varepsilon \tau_{x1} = - \frac{1}{\beta y^2} \left(\frac{31}{100} u_{\infty}^2 - \frac{17}{50} v_{\infty}^2 + \frac{1}{28} u_{\infty} v_{\infty} \right) \sqrt{\frac{\beta y \kappa}{2}} \quad (3.9)$$

$$\varepsilon \tau_{y1} = - \frac{1}{\beta y^2} \left(\frac{19}{50} u_{\infty}^2 - \frac{37}{100} v_{\infty}^2 + \frac{19}{420} u_{\infty} v_{\infty} \right) \sqrt{\frac{\beta y \kappa}{2}} \quad (3.10)$$

From these expressions for the correction to the bottom stress, it can be seen that there is again a substantial veering in the correction. The corrections are of the order of $\varepsilon/3$ times the shear stress in the absence of upwelling. The importance of the correction decays quickly with distance from the equator. If applied at the equator (3.9) and (3.10) exhibit a singularity. For the derivation of (3.9) and (3.10) to be valid, $|\varepsilon|$ must be less than unity. Thus the model is only valid for

$$|y| \gg \left(\frac{u_{\infty}^2 + v_{\infty}^2}{\beta^{1/2}} \right)^{1/4} \quad (3.11)$$

As suggested by the work of MCKEE (see GILL, 1975), on wind forced equatorial flows, (3.9) and (3.10) may be extended into the region spanning the equator by writing them in modified form as

$$\begin{aligned} \epsilon \tau_{x1} &= \max \left\{ \frac{\beta c}{r^2 + \beta^2 y^2} \left(u_{\infty} + v_{\infty} \frac{\beta y}{(r^2 + \beta^2 y^2)^{1/2}} \right) \right\} \tau_{x0} \\ &\quad \left\{ \begin{array}{l} -1 \\ -1 \end{array} \right\} \quad (3.12) \\ \epsilon \tau_{y1} &= \max \left\{ \frac{\beta c}{r^2 + \beta^2 y^2} \left(v_{\infty} + u_{\infty} \frac{\beta y}{(r^2 + \beta^2 y^2)^{1/2}} \right) \right\} \\ &\quad \left\{ \begin{array}{l} \tau_{x0}/\tau_{y0} \\ \tau_{y0} \end{array} \right\} \quad (3.13) \end{aligned}$$

where c is a constant of approximate value $1/3$ and r is characteristic of a Rayleigh friction factor. The Rayleigh friction has not been introduced until now because earlier inclusion would have made the problem unmanageable. Furthermore, as a Rayleigh friction is of little physical basis, its mode of inclusion is slightly arbitrary. In these expressions the value of c has been obtained as an approximation to $31/100$, $17/50$, $19/50$ and $37/100$ in (3.9) and (3.10). Interactions between u_{∞} and v_{∞} have been ignored as suggested by their small coefficients in (3.9) and (3.10). τ_{x0} has been determined from (3.3). The corrections have been restricted in magnitude so that they cannot reverse the shear stress direction. Using this parameterisation we are now in a position to study the effect of this frictionally induced upwelling on the across-equatorial flow. Notice that although the correction to the bottom stress is of higher order in velocity magnitude than is usually retained in basin studies such as those of GROVES and NIEMEYER (1975) for low latitudes and FANDRY (1981) for middle latitudes, it should not be neglected in equatorial situations because its coefficient has a "near" singularity at the equator.

4. MODEL OF CROSS-EQUATORIAL FLOW

Having developed albeit a simple model, to obtain a parameterisation of the correction to the bottom stress from the secondary circulation, it is useful to look at what effects it may have on cross-equatorial flow. In this section cross-equatorial flow is considered in a "near unbounded" basin of uniform depth H . The words "near unbounded" are used because although the boundaries of the basin are neglected here, they are essential for achieving the return flow required by the secondary circulation. The vertically averaged steady state equations of motion are

$$-\beta y V = -\frac{\partial p}{\partial x} - rU + \frac{\tau_x}{H} + \frac{X}{H} \quad (4.1)$$

$$\beta y U = -\frac{\partial p}{\partial y} - rV + \frac{\tau_y}{H} + \frac{Y}{H} \quad (4.2)$$

$$\frac{\partial U}{\partial x} + \frac{\partial V}{\partial y} = 0 \quad (4.3)$$

where (X, Y) and (U, V) are respectively the constant kinematic wind stress and the vertically averaged velocity field. The small Rayleigh friction factor r is chosen to be the same as that used in (3.12) and (3.13). As τ_x and τ_y can be zero according to the formulation contained in (3.12) and (3.13), the small Rayleigh friction factor times H serves as a heuristically chosen minimum bottom drag. The present study does not press the formulation to this limit and so the Rayleigh friction can be neglected in (4.1)

and (4.2). The terms $\frac{1}{H} \int w \frac{\partial u}{\partial z} dz$ and $\frac{1}{H} \int w \frac{\partial v}{\partial z} dz$

can be neglected. This can be seen by integrating the terms by parts. Then using the continuity equation to identify the terms as being of the order of the small horizontal advective acceleration terms which are also commonly neglected. The velocity field (U, V) is approximately equal to the far field velocity field (u_{∞}, v_{∞}) used earlier. This assumption is used throughout the remainder of this study.

An examination of the results of GROVES and NIEMEYER (1975) shows that in the region of interest here ($4^{\circ} N$ to $4^{\circ} S$ on the Sunda Shelf) the dominant terms in (4.1) and (4.2) are the pressure gradient and bottom and wind stresses. Thus we assume for this study that

$$0 = -\frac{\partial p}{\partial x} + \frac{\tau_x}{H} + \frac{X}{H} \quad (4.4)$$

$$0 = -\frac{\partial p}{\partial y} + \frac{\tau_y}{H} + \frac{Y}{H} \quad (4.5)$$

Of course this ignores the turning effect of the Coriolis force at larger latitudes but it is a useful approximation to make.

We consider the particular case in which the velocity field is independent of x . Thus from the continuity equation (4.3), V is uniform. Differentiating (4.5) with respect to x and using (4.4), it follows that $\frac{\partial p}{\partial x}$ is a constant which we define to be A . Thus

for a given A and V , (4.4) alone can be used to determine U as a function of y . It follows that U is such that $\tau_x (= HA - X)$ is a constant everywhere. For consistency with GROVES and NIEMEYER (1975), rather than arbitrarily define a value of x , the present study will use the familiar drag relation

$$\tau_{x0} = -D U \sqrt{U^2 + V^2} \quad (4.6)$$

$$\tau_{y0} = -D V \sqrt{U^2 + V^2} \quad (4.7)$$

where $D = .004$ as used by GROVES and NIEMEYER. As veering at the order ϵ^0 level is produced by the

local Coriolis parameter, there is no need to allow for any veering in this equatorial case. This formulation is generally considered to be satisfactory even when there is bottom topography and there is little reason to dispute its applicability here. Several authors, for example FANDRY (1983), have related D to κ . Using (3.12) and (4.6) it follows that

$$U = \text{sgn}(X - HA - C_{\text{or}}) \left(\left(\frac{X - HA - C_{\text{or}}}{D} \right)^2 + \frac{1}{4} V^4 \right)^{1/2} - \frac{1}{2} V^2 \quad (4.8)$$

where $C_{\text{or}} = 0$ for the order ε^0 solution. This gives a constant value for U which we write as U_0 . The

order ε^1 $\left(= \frac{\beta(U_0^2 + V^2)^{1/2}}{r^2} \right)$ solution is also given by (4.8) but with

$$C_{\text{or}} = \frac{\beta c}{r^2 + \beta^2 y^2} \left(U_0 + V \frac{\beta y}{(r^2 + \beta^2 y^2)^{1/2}} \right) (X - HA) \quad (4.9)$$

Veering is possible at the order ε^1 level because at this level the gradient of the Coriolis parameter is important.

If U and V are of the same sign, the westward correction to U is the greatest for $y > 0$ that is north of the equator. If U and V are of opposite sign the westward correction to U is greatest south of the equator. This latter case is that applicable to the Sunda Shelf. For this case the western boundary current is most strongly fed in the Southern Hemisphere although some feeding may occur in the Northern Hemisphere. Thus during the South-East Monsoon, June-August, when the flow is to the North-East, the contrast between the across equatorial boundary current and the general flow might be expected to be at its most prominence. This idea is (albeit weakly) supported by fig. 1.

A particle of water follows a path given by

$$\frac{dx}{dy} = \frac{U}{V} \quad (4.10)$$

Fig. 4 shows the path of particles in the case of $r = 10^{-6} \text{ s}^{-1}$, $\beta = 2 \times 10^{-11} \text{ m}^{-1} \text{ s}^{-1}$, $(X-HA)/D = -0.35 \text{ m}^2 \text{ s}^{-2}$ and $V = 0.5 \text{ ms}^{-1}$ obtained by a Runge-Kutta procedure. The deviation from the

line $x = y \frac{U_0}{V}$ is that caused by the correction to the bottom stress. This deviation is to the west as expected.

For simplicity the above model has neglected bottom topography. Bottom topography cannot be neglected in any detailed simulation. However, GROVES and NIEMEYER retained it in their model and found it could not produce the observed boundary current. Thus, it would seem justifiable to neglect

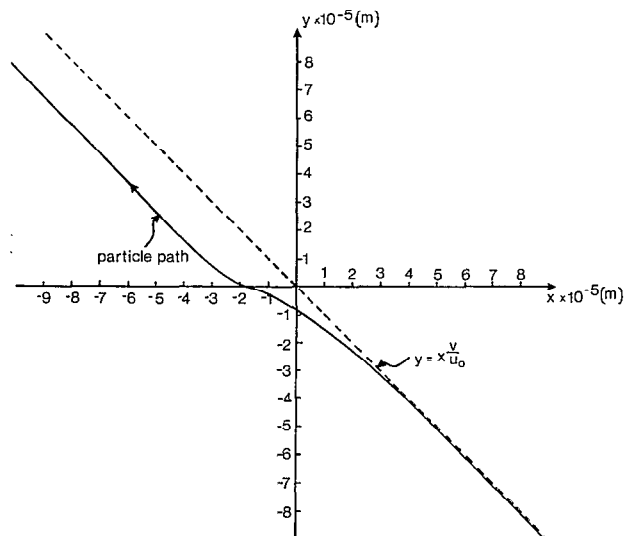


Fig. 4. — Typical predicted particle path for across-equatorial flow in a shallow wind driven sea as calculated using (4.10). Dashed line indicates the path when the correction is ignored. Notice the tendency for the flow to deviate to the west in the general vicinity of the equator.

Trajectoire d'une particule franchissant l'Équateur, dans une mer peu profonde entraînée par le vent, calculée d'après la relation (4.10). La ligne tiretée indique la trajectoire en l'absence de correction. Noter la tendance du courant à dévier vers l'Ouest au voisinage de l'Équateur.

the topography in the present search for a mechanism that can produce the observed irregularity in the flow.

From this simple model it may be expected that in a basin there would be a strong flow on western boundaries such as appears to be observed near Singapore. The proposed mechanism for this flow is quite different to that usually given for the much larger mid-latitude western boundary currents such as the Kurishio and Gulf Stream.

CONCLUSIONS

A simple theory has been proposed to explain the existence of the western boundary current near Singapore. It is well known that the absence of a strong geostrophic balance in equatorial regions enables large vertical velocities. Furthermore β -effects encourage such motion (GILL, 1975). Thus if the bottom stress is eastward, the upward motion within the bottom boundary layer which it induces, thickens the boundary layer. The results is a decreased bottom stress. Similarly, if the bottom stress is westward the downward motion induced within the boundary layer increases the bottom stress. The

result is a westward correction to the bottom stress forcing water to the west and creating an equatorial western boundary current. In a depth integrated model, the vertical advection of momentum associated with the boundary layer is of the order of the often neglected horizontal advective accelerations. However, the correction to the bottom stress by the above mechanism is only limited by the choice of Rayleigh friction used to overcome the usual equatorial singularity. This small Rayleigh friction corresponds to a heuristic lower limit on the bottom drag which the flow can experience.

The model used here is based on extremely

elementary boundary layer physics. Thus it should be seen as little more than an expression of these physical ideas in a slightly more rigorous manner. Nevertheless the effect appears to be real and provides yet another example of the unusual phenomena which can occur in tropical oceans.

ACKNOWLEDGEMENTS

I am grateful to Misses G. BURT and J. CAMPBELL for their help in preparing this manuscript.

*Manuscrit reçu au Service des Éditions de l'O.R.S.T.O.M.
le 14 février 1984*

REFERENCES

- BARCILON (V.), 1965. — Stability of a non-divergent Ekman layer. *Tellus*, 17 : 53-68.
- FANDRY (C.), 1981. — Development of a numerical model of tidal and wind-driven circulation in Bass Strait. *Aust. J. Mar. Freshwat. Res.*, 32 : 9-29.
- FANDRY (C.), 1983. — A model for the three-dimensional structure of the wind-driven and tidal circulation in Bass Strait. *Aust. J. Mar. Freshwat. Res.*, 34 : 121-141.
- FORRISTALL (G. Z.), HAMILTON (R. C.) and CARDONE (V. J.), 1977. — Continental shelf currents in Tropical Storm Delia : Observations and theory. *J. Phys. Oceanogr.*, 7 : 532-546.
- GILL (A. E.), 1975. — Models of equatorial currents. In: *Numerical Models of Ocean Circulation*. National Academy of Science : 181-203.
- GREENSPAN (H. P.), 1969. — *The Theory of Rotating Fluids*. Cambridge, 328 p.
- GROVES (G. W.) and NIEMEYER (G.), 1975. — A numerical simulation of wind-driven water circulation on the Sunda shelf. *Mar. Res. Indon.*, 14 : 31-47.
- HANSEN (W.), 1962. — Hydrodynamical methods applied to oceanographic problems. Proceeding of the Symposium on mathematical-hydrodynamical methods of physical oceanography. *Mitt. Inst. Meeresk., Hamburg*, 1 : 25-34.
- HSUEH (Y.) and O'BRIEN (J. J.), 1971. — Steady coastal upwelling induced by an along-shore current. *J. Phys. Oceanogr.*, 1 : 180-186.
- POLLARD (R. T.), 1977. — Observations and models of the structure of the upper ocean. In: E. B. KRAUS (Ed.), *Modelling and Prediction of the Upper Layers of the Ocean*. Pergamon : 102-117.
- SCOTT (J. T.) and CSANADY (G. T.), 1976. — Nearshore currents off Long Island. *J. Geophys. Res.*, 81 : 5401-5409.
- SMITH (N. P.), 1978. — Longshore currents on the fringe of Hurricane Anita. — *J. Geophys. Res.*, 83 : 6047-6051.
- WYRTKI (K.), 1961. — Physical oceanography of the Southeast Asian waters. *Naga Rep.*, 2 : 1-395.